Journal of Organometallic Chemistry, 388 (1990) 233–242
Elsevier Sequoia S.A., Lausanne – Printed in The Netherlands
JOM 20754

Isonitrile-containing platinum-gold phosphine clusters

R.P.F. Kanters, P.P.J. Schlebos, J.J. Bour, J. Wijnhoven, E. van den Berg, and J.J. Steggerda *

Inorganic Chemistry Department, University of Nijmegen, 6525 ED Nijmegen (The Netherlands)

(Received December 7th, 1989)

Abstract

Pt–Au-phosphine clusters with an isonitrile ligand on Pt or on both Pt and Au can be synthesized from $[Pt(AuPPh_3)_8]^{2+}$. The reaction of one equivalent of RNC (R = i-Pr,t-Bu) with $[Pt(AuPPh_3)_8]^{2+}$ results in the addition of RNC to the central Pt, to form $[Pt(RNC)(AuPPh_3)_8]^{2+}$. The addition of an excess of RNC results in the replacement of one of the Au-bonded PPh_3 ligands to give $[Pt(RNC)(AuRNC)(AuPPh_3)_7]^{2+}$. Treatment of $[Pt(CO)(AuPPh_3)_8]^{2+}$ with an excess of RNC does not result in displacement of the Pt-bonded CO ligand but only one of the Au-bonded PPh_3 ligands, to yield $[Pt(CO)(AuRNC)(AuPPh_3)_7]^{2+}$. Ag adducts of all of these compounds can be prepared by the addition of one equivalent of $AgNO_3$.

The compounds have been characterized by IR and NMR (^1H, ^{31}P and ^{195}Pt) spectroscopy and elemental analysis. The structures are thought to be isostructural with the reported $[Pt(AgNO_3)_x(CO)_y(AuPPh_3)_8](NO_3)_2$ compounds, with x, y = 0, 1. NMR and IR data for these clusters are compared, and observed trends analysed in terms of σ-donor and π-acceptor considerations. A fragment molecular orbital analysis of $[Pt(CO)(AuPPh_3)_8](NO_3)_2$ is presented. The changes in bonding characteristics upon addition of CO to $[Pt(AuPPh_3)_8](NO_3)_2$ are examined and the decrease of the radial $^2J(Pt–P)$ coupling constant is explained in terms of the results.

Introduction

We previously reported on the synthesis, characterization, and reactivity of gold phosphine cluster compounds containing isonitriles as peripheral ligands [1,2]. The isoelectronicity and isostructurality of the starting $[Au(AuPPh_3)_8]^{3+}$ cluster with the mixed-metal $[Pt(AuPPh_3)_8]^{2+}$ cluster prompted us to investigate the reactions of the latter cluster compound with isonitriles. From the reaction of $[Pt(AuPPh_3)_8]^{2+}$ with CO, to give the addition product $[Pt(CO)(AuPPh_3)_8]^{2+}$ [3], which does not have an analogue in homonuclear gold cluster chemistry, it is clear that although the bonding description of these σ clusters is the same, the reactivities and stabilities of the compounds can be different.

The nucleophilic addition reaction of a two-electron donating group to the center of a toroidal $(S^{\sigma})^2(P^{\sigma})^4$ cluster is demonstrated by the following reactions [3,4]:

$$[Pt(AuPPh_3)_8]^{2+} + CO \longrightarrow [Pt(CO)(AuPPh_3)_8]^{2+} \quad (1)$$

$$[Au(AuPPh_3)_7]^{2+} + PPh_3 \longrightarrow [Au(PPh_3)(AuPPh_3)_7]^{2+} \quad (2)$$

It has been shown by Vollenbroek [5] that addition of a Lewis base to an $(S^{\sigma})^2(P^{\sigma})^6$ cluster compound results in the replacement of the ligands on the peripheral Au atoms:

$$Au(AuL)_7(AuSCN)_3 + nL' \longrightarrow Au(AuL)_{7-n}(AuL')_n(AuSCN)_3 \quad (3)$$

($L = PPh_3$ and $L' = P(p\text{-}ClC_6H_4)_3$)

The electrophilic addition of a d^{10} cation to an $(S^{\sigma})^2(P^{\sigma})^4$ or $(S^{\sigma})^2(P^{\sigma})^6$ cluster compound has also been reported [6].

$$[Pt(AuPPh_3)_8]^{2+} + Ag^+ \longrightarrow [Pt(Ag)(AuPPh_3)_8]^{3+} \quad (4)$$

$$[Pt(CO)(AuPPh_3)_8]^{2+} + Ag^+ \longrightarrow [Pt(Ag)(CO)(AuPPh_3)_8]^{3+} \quad (5)$$

Such substitution and addition reactions allow synthesis of a variety of isonitrile-containing cluster compounds. Comparison of NMR and IR data can provide a better understanding of the electronic interactions determining the bonding in this type of cluster compound.

In this paper we report the synthesis and characterization of $[Pt(L)(AuPPh_3)_8](NO_3)_2$, $[Pt(AgNO_3)(L)(AuPPh_3)_8](NO_3)_2$, $[Pt(L)(AuRNC)(AuPPh_3)_7](NO_3)_2$ and $[Pt(AgNO_3)(L)(AuRNC)(AuPPh_3)_7](NO_3)_2$ compounds with L = CO, RNC; R = i-Pr or t-Bu.

Experimental

Measurements

C, H and N analyses were carried out in the Micro Analytical Department of the University of Nijmegen. Pt, Ag, Au and P analyses were performed on a 200 ICPAE spectrophotometer. ^{31}P proton decoupled NMR spectra were recorded at 298 K on a Bruker WM200 spectrometer, operating at 81.02 MHz for ^{31}P, for CD_2Cl_2 solutions containing TMP as internal reference. ^1H spectra were recorded at 298 K on the same spectrometer at 200.13 MHz. ^{195}Pt-NMR spectra were recorded at room temperature on the same spectrometer at 43.02 MHz, with a solution of $PtCl_6^{2-}$ in D_2O as external reference. Infrared spectra were recorded on a Perkin Elmer 1720-X spectrophotometer with CsI pellets.

Preparation of the compounds

$[Pt(AuPPh_3)_8](NO_3)_2$, [7] $[Pt(CO)(AuPPh_3)_8](NO_3)_2$, [3] $[Pt(AgNO_3)(AuPPh_3)_8](NO_3)_2$ and $[Pt(AgNO_3)(CO)(AuPPh_3)_8](NO_3)_2$ [6] were prepared by published methods. The other reagents were obtained from commercial sources and used without further purification.

$[Pt(RNC)(AuPPh_3)_8](NO_3)_2$ (R = i-Pr, t-Bu). A solution of 100 mg of $[Pt(AuPPh_3)_8](NO_3)_2$ in 5 ml of CH_2Cl_2, was cooled to $-20\,^{\circ}C$ and exactly one equivalent of the isonitrile was added with vigorous stirring. The mixture was allowed to warm to room temperature.

$[Pt(L)(AuRNC)(AuPPh_3)_7](NO_3)_2$ (L = CO, CN-i-Pr, CN-t-Bu; R = i-Pr, t-Bu). To a solution of 100 mg of $[Pt(L)(AuPPh_3)_8](NO_3)_2$ in 5 ml of CH_2Cl_2, a slight excess of RNC was added with vigorous stirring. The mixture was kept at room temperature for 0.5 h.

$[Pt(AgNO_3)(RNC)(AuPPh_3)_8](NO_3)_2$ (R = i-Pr, t-Bu). This compound was prepared by two methods. One involved addition of exactly one equivalent of $AgNO_3$ in methanol to a methanolic solution of $[Pt(RNC)(AuPPh_3)_8](NO_3)_2$, and the other that of one equivalent of RNC to a methanolic solution of $[Pt(AgNO_3)(AuPPh_3)_8](NO_3)_2$, with vigorous stirring in both cases.

$Pt(AgNO_3)(L)(AuRNC)(AuPPh_3)_7](NO_3)_2$ (L = CO, CN-i-Pr; R = t-Bu, i-Pr). These compounds were prepared by the addition of one equivalent of $AgNO_3$ to $[Pt(L)(AuRNC)(AuPPh_3)_7](NO_3)_2$ or that of a small excess of RNC to $[Pt(AgNO_3)(L)(AuPPh_3)_8](NO_3)_2$, in both cases in methanol solution with vigorous stirring.

In all the preparations described above, the product mixtures were poured into diethyl ether. The products were filtered off and recrystalized by slow diffusion of diethyl ether into methanolic solutions of the compounds. All yields were nearly quantitative. All gave good elemental analyses. The physical data are presented later below.

The $[Pt(AgNO_3)_n(RNC)(AuR'NC)(AuPPh_3)_7](NO_3)_2$ ($n = 0, 1$; R' = t-Bu, i-Pr) clusters were also prepared by the addition of a large excess of R'NC to a solution of $[Pt(AgNO_3)_n(RNC)(AuRNC)(AuPPh_3)_8](NO_3)_2$ in methanol.

The addition of an excess of RNC to a CH_2Cl_2 solution of $[Pt(L)(AuPPh_3)_8]^{2+}$ gave the product in which only one PPh_3 ligand on the peripheral gold atoms has been replaced. No reaction was observed when a solution of $[Pt(L)(AuPPh_3)_8]^{2+}$ was exposed to carbon monoxide, and there was no displacement of the ligand bonded to the central Pt atom.

Results

The observed transformations are shown below:

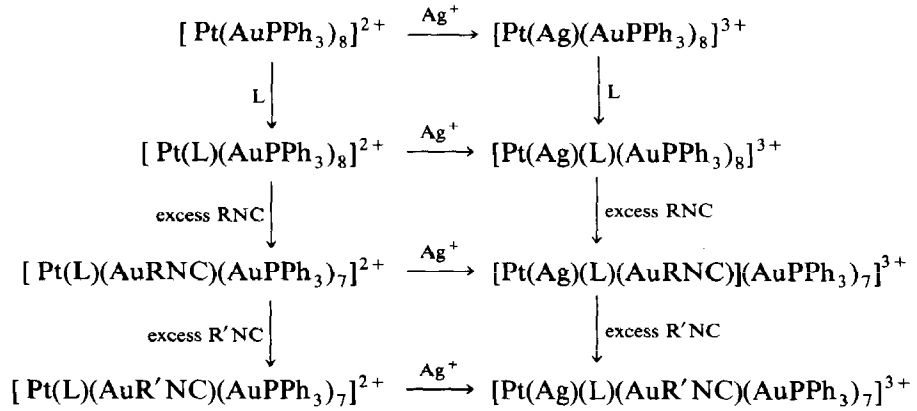

(L = CO, or RNC; R, R' = i-Pr or t-Bu)

Table 1

Infrared data for the series $[Pt(L)(AuRNC)(AuPPh_3)_7](NO_3)_2$ and $[Pt(L)(AuPPh_3)_8](NO_3)_2$ (L = CO, CN-i-Pr, CN-t-Bu; R = i-Pr, t-Bu; all ν in cm^{-1})

Ligand bonded to		ν(CO)	ν(PtC≡N)	ν(AuC≡N)
Pt	Au			
CO	PPh_3	1939	–	–
CO	CN-i-Pr	1954	–	2191
CO	CN-t-Bu	1951	–	2180
CN-i-Pr	PPh_3	–	2104	–
CN-i-Pr	CN-i-Pr	–	2108	2185
CN-i-Pr	CN-t-Bu	–	2107	2174
CN-t-Bu	PPh_3	–	2091	–
CN-t-Bu	CN-i-Pr	–	2098	2184
CN-t-Bu	CN-t-Bu	–	2100	2174

Table 2

NMR-data for the series $[Pt(L)(AuRNC)(AuPPh_3)_7](NO_3)_2$ and $[Pt(L)(AuPPh_3)_8](NO_3)_2$ (L = CO, CN-i-Pr, CN-t-Bu; R = i-Pr, t-Bu; for ^1H NMR only the chemical shifts of the methyl group are given; all shifts in ppm, coupling in Hz)

Ligand bonded to		^{31}P		^1H		^{195}Pt	
Pt	Au	δ	^2J(Pt–P)	δ(PtCNR)	δ(AuCNR)	δ	^2J(P–Pt)
–	PPh_3	55.3	497	–	–	−4528.3	497
CO	PPh_3	51.3	391	–	–	−5456.7	391
CO	CN-i-Pr	53.2	372	–	0.94	−5621.9	373
CO	CN-t-Bu	52.8	373	–	0.97	−5625.4	373
CN-i-Pr	PPh_3	50.4	400	0.85	–	−5271.0	400
CN-i-Pr	CN-i-Pr	51.9	379	0.61	0.91	−5423.7	380
CN-i-Pr	CN-t-Bu	51.5	380	0.60	0.92	−5423.2	380
CN-t-Bu	PPh_3	49.8	403	0.85	–	−5287.1	403
CN-t-Bu	CN-i-Pr	51.4	382	0.68	0.86	−5435.3	382
CN-t-Bu	CN-t-Bu	51.1	383	0.70	0.91	−5435.3	383

Table 3

Infrared data for the series $[Pt(AgNO_3)(L)(AuRNC)(AuPPh_3)_7](NO_3)_2$ and $[Pt(AgNO_3)(L)(AuPPh_3)_8](NO_3)_2$ (L = CO, CN-i-Pr; R = i-Pr, t-Bu; ν in cm^{-1})

Ligand bonded to		IR		
Pt	Au	ν(CO)	ν(PtC≡N)	ν(AuC≡N)
CO	PPh_3	1961	–	–
CO	CN-i-Pr	1973	–	2209
CO	CN-t-Bu	1973	–	2201
CN-i-Pr	PPh_3	–	2119	–
CN-i-Pr	CN-i-Pr	–	2132	2199
CN-i-Pr	CN-t-Bu	–	2134	2193

Table 4

NMR data for the series $[Pt(AgNO_3)(L)(AuRNC)(AuPPh_3)_7](NO_3)_2$ and $[Pt(AgNO_3)(L)(AuPPh_3)_8](NO_3)_2$ (L = CO, CN-i-Pr; R = i-Pr, t-Bu) in EtOH at 328 K (all shifts in ppm, coupling in Hz)

Ligand bonded to		^{31}P			^{1}H	
Pt	Au	δ	^{2}J(Pt–P)	^{3}J(Ag–P)	δ(PtCNR)	δ(AuCNR)
–	PPh_3	57.0	453	19	–	–
CO	PPh_3	54.3	366	17	–	–
CO	CN-i-Pr	54.4	355	16	–	0.86
CO	CN-t-Bu	54.1	362	16	–	0.87
CN-i-Pr	PPh_3	51.4 [a]	350	–	0.32	–
CN-i-Pr	CN-i-Pr	52.7	365	12	0.50	0.86
CN-i-Pr	CN-t-Bu	52.4	360	12	0.46	0.88

[a] Data at 298 K because of instability of the cluster at higher temperature.

The spectroscopic data obtained for the $[Pt(L)(AuRNC)(AuPPh_3)_7](NO_3)_2$ and $[Pt(L)(AuPPh_3)_8](NO_3)_2$ (L = CO, CN-i-Pr, CN-t-Bu; R = i-Pr, t-Bu) clusters are presented in Tables 1 and 2. The data obtained for the $[Pt(AgNO_3)(L)(AuRNC)(AuPPh_3)_7](NO_3)_2$ and $[Pt(AgNO_3)(L)(AuPPh_3)_8](NO_3)_2$ (L = CO, CN-i-Pr; R = i-Pr, t-Bu) clusters are presented in Tables 3 and 4.

Since the ^{31}P-NMR spectra of the Ag-containing clusters showed broad resonances at room temperature, the spectra were recorded at 328 K with ethanol solutions in order to obtain sharper lines showing the ^{3}J(Ag–P) coupling. The lines were still to broad to reveal the separate couplings with the two silver isotopes.

Discussion

Synthesis of the compounds

From the observered transformations it is clear that the addition of the first equivalent of a two-electron donating group results in the completion of the $(S^{\sigma})^2(P^{\sigma})^6$ electron configuration by coordination to the central metal atom. Use of more than one equivalent of RNC results in the replacement of a peripheral PPh_3 ligand. Even use of a large excess of the RNC and prolonged exposure times results in only a single substitution. No displacement of the Pt-bonded ligand was observed.

A possible explanation may be that the driving force for the replacement is the relaxation of the steric hindrance when the bulky phosphine ligand is substituted for a smaller isonitrile. Subsequent substitutions will not occur because the singly-substituted cluster already has small steric hindrance.

With gold cluster compounds use of an excess of RNC leads to the total breakdown of the cluster. The stability of the mixed platinum-gold cluster towards excesses of RNC can be attributed to the fact that the central metal atom in this case can not migrate to the surface. In gold cluster compounds on the other hand, the central gold atom bearing the added RNC ligand can exchange positions with a peripheral $AuPPh_3$ ligand. This will cause a strong steric hindrance for the PPh_3 bonded to the new central metal atom, resulting in the loss of this phosphine. The resulting cluster has again an $(S^{\sigma})^2(P^{\sigma})^4$ configuration and can be further attacked

by Lewis bases. Another reason for the instability of the gold clusters towards isonitriles may be the existence of the following, well known, equilibrium [8]:

$$[Au(AuPPh_3)_7]^{3+} \rightleftharpoons [Au(AuPPh_3)_7]^{2+} + AuPPh_3^{+}$$

which is not observed for the isoelectronic $[Pt(AuPPh_3)_8]^{2+}$ cluster. The $[Au(AuPPh_3)_7]^{2+}$ cluster is known to be a reactive intermediate in gold cluster chemistry.

IR data

The assignment of the CN stretching frequencies in the clusters containing two isonitriles was made by comparison of the data observed for the clusters with CO on the central atom and only a Au-bonded RNC group. In all cases the stretching frequency for the ligand bonded to the central atom is lower than that for the peripheral ligands. The high CN stretching frequency of the RNC bonded to the periphery is a consequence of the small π^* back-donation ability of the mainly *sp* hybridized peripheral gold atoms. The central metal atom has larger *p* atomic orbital contributions in the HOMO orbitals, and can therefore contribute more to the π^* back-donation. This effect has also been observed for the $[Pt(CN)(AuCN)(AuPPh_3)_7]^+$ cluster [9].

The addition of a Ag atom results in an increase in the stretching frequencies. This effect is larger for the ligand bonded to the central atom (15–27 cm^{-1}) than for the ligand on the periphery (15–21 cm^{-1}). The increase is caused by the decrease in the $\pi^\star$ donating ability of the metal atoms arising from the electron withdrawing effect of the Ag atom.

Another observed trend is the increase in the ν(CN) or ν(CO) frequencies for the group bonded to the central metal atom when a σ donating phosphine is replaced by a RNC ligand, which is a π-acceptor ligand with smaller σ donation ability. This effect is the strongest in the silver containing clusters. The value of ν(CN) for the peripheral RNC ligand is almost the same in respect of whether the isonitrile on the center is CN-i-Pr or CN-t-Bu. The frequency is higher when a CO is bonded to the center, showing that the π acceptor abilities of the two isonitriles are almost the same, but smaller than that of CO.

NMR data

Chemical shifts

The addition of a two-electron donating group to the central metal atom of an $(S^\sigma)^2(P^\sigma)^4$ clusters results in a considerable fall in the resonance frequencies for the ^{31}P atoms of the phosphine ligands as well as for the 195 Pt atom in the center of the cluster, probably because of the increased electron density in the cluster, which results in a larger contribution by the diamagnetic term in the shielding. Also the decrease of the asymmetry in the electron distribution around the central atom results in a decrease of the paramagnetic term and an increase in the total shielding. There is a significant difference in the magnitude of the shift of the ^{195}Pt resonance to low frequency on going from the CO to the isonitrile clusters. This cannot be attributed to the σ-donor ability of the CO ligand, since this is smaller than that of RNC.

The shielding of the non-hydrogen nuclei is influenced strongly by the paramagnetic term in the total shielding. Since this paramagnetic shielding involves excitation energies, the differences in the contribution of this term to the total shielding is difficult to predict. This is also shown by the fact that the replacement of a peripheral PPh_3 ligand by a RNC group causes an increase in the shielding of Pt, as well as the methyl hydrogens of the RNC bonded to this atom and that the shielding of the phosphine-phosphorus atoms is decreased.

The ^1H NMR data show that the hydrogen chemical shifts of the CH_3 groups in the RNC ligands depend mainly on the position of the groups in the cluster. The methyl protons are more shielded when the RNC is bonded to the central Pt, suggesting that bonding to the central atom causes a larger *s* electron density on the hydrogen than bonding to a peripheral Au atom.

Radial coupling

The values of the platinum-phosphorus coupling constants enable us to compare the trends in radial bonding characteristics of clusters with and without π acid ligands on the centre or periphery. To obtain an understanding of the orbital interactions involved in the addition of a π-acid ligand to $[Pt(AuPPh_3)_8]^{2+}$ we first analysed the changes in the molecular orbitals in the frontier region when the geometry is changed from toroidal (idealized S_8) to hemispherical (C_2). The hemispherical geometry is that of the $Pt(AuPPh_3)_8$ frame as found in $[Pt(CO)(AuPPh_3)_8]^{2+}$. These analyses draw heavily on the previous MO studies on gold cluster compounds [10–13], and the mode of calculation and the parameters used are similar to those used in those studies. The bond lengths used in these EHMO calculations are the average distances revealed by the X-ray structure determinations. For $[Pt(AuPPh_3)_8]^{2+}$ these are 2.64 for the Pt–Au and 2.27 Å for Au–P, [7] and for $[Pt(CO)(AuPPh_3)_8]^{2+}$ 2.67 and 2.30 Å,respectively. Pt–C = 1.90 and C–O = 1.13 Å. The structure and numbering of the Au sites is shown in Fig. 1.

The effect of the geometrical change is shown in the left hand side of Fig. 2. On the extreme left of this figure we see the energy levels of the cluster skeleton orbitals for the toroidal $Pt(AuPPh_3)_8$ cluster. In order of increasing energy these are the $a(S^\sigma)$, $e_1(P^\sigma_{x,y})$, $b(P^\sigma_z)$, $e_2(D^\sigma_{x^2-y^2,xy})$, $e_3(D^\sigma_{xz,yz})$ and $a(D^\sigma_{z^2})$. It is obvious that the

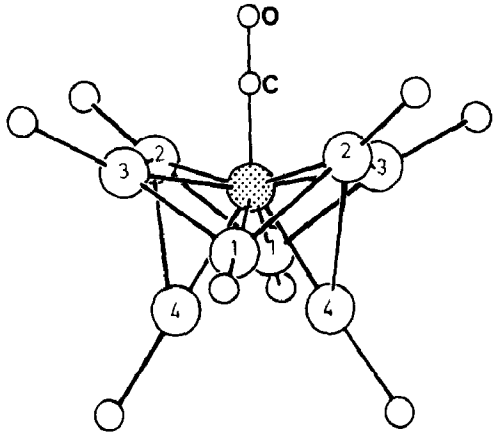

Fig. 1. Structure and labelling of the $[Pt(CO)(AuPPh_3)_8]^{2+}$ cluster.

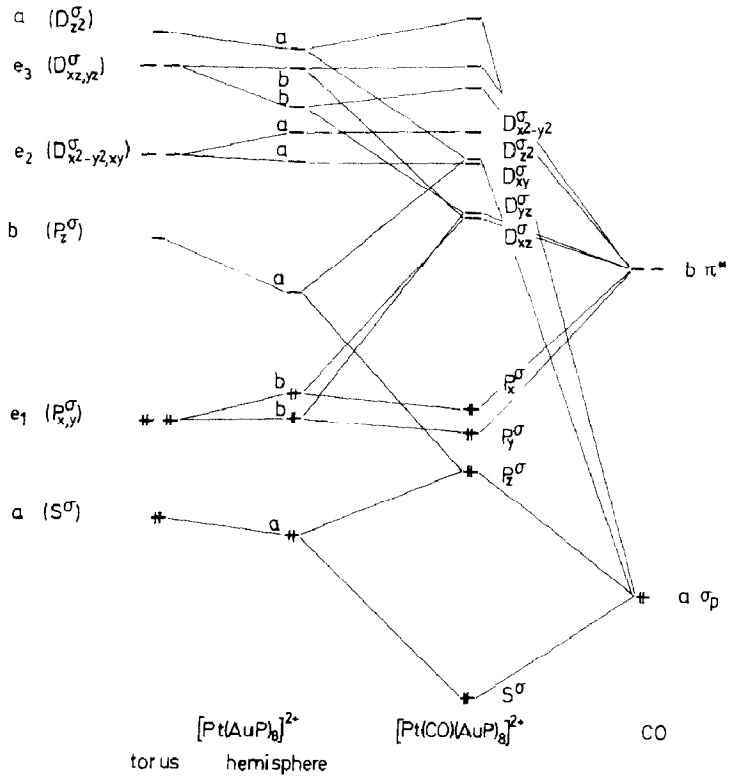

Fig. 2. Molecular orbital interaction diagrams. On the left hand side is shown the diagram for the toroidal and hemispherical $[Pt(AuPPh_3)_8]^{2+}$. On the right hand side is shown the fragment orbital interaction diagram between the CO and the hemispherical $[Pt(AuPPh_3)_8]^{2+}$ cluster.

closed shell requirements will be fulfilled by an $(S^{\sigma})^2(P^{\sigma})^4$ electron configuration. This results in a HOMO–LUMO gap $(e_1(P^{\sigma}_{x,y}) - b(P^{\sigma}_{z}))$ of 2.31 eV.

When the geometry is changed to hemispherical we see that all degeneracies are lost. The most important change involves the lowering of the P^{σ}_{z} energy by 0.69 eV. In addition the P^{σ}_{x} energy is increased by 0.37 eV, resulting in a HOMO–LUMO gap of only 1.23 eV. The total energy increases by 1.27 eV, showing that the hemispherical arrangement is less favourable, unless the LUMO becomes involved in bonding.

On the right hand side of Fig. 2 the fragment molecular orbital interaction between the $[Pt(AuPPh_3)_8]^{2+}$ hemisphere and the CO moiety is shown. The only orbitals of CO in this figure are the $\sigma_p(a)$ and $\pi^{\star}(b)$ orbitals. The σ_s, $\sigma_s^{\star}$ and π orbitals are too low in energy, and the $\sigma_p^{\star}$ too high to participate. The a orbital interacts strongly with the $a(S^{\sigma})$ and $a(P^{\sigma}_{z})$ skeletal molecular orbitals. This results in a new bonding P^{σ}_{z} orbital and an electron configuration of $(S^{\sigma})^2(P^{\sigma})^6$. The $\pi^{\star}(b)$ orbitals combine with the P^{σ}_{x} and P^{σ}_{y} skeletal orbitals. The energy lowering of these orbitals is only small because of the small overlap. The $\pi^{\star}$ orbitals interact more strongly with the D^{σ} antibonding orbitals, lowering especially the D^{σ}_{xz} and D^{σ}_{yz} orbitals. Because of these interactions the $\pi^{\star}$ orbitals become slightly occupied (0.69 $\bar{e}$). The HOMO–LUMO gap is 2.41 eV.

The data in Table 5 show that the introduction of the CO ligand causes a redistribution of electron density. In the absence of this ligand the sites closest to

Table 5

Radial metal–metal overlap populations

	$Pt(AuPPh_3)_8$		$Pt(CO)(AuPPh_3)_8$
	toroidal	hemisphere	
Pt-Au1	0.2569	0.2640	0.2387
Pt-Au2	0.2569	0.2094	0.2606
Pt-Au3	0.2569	0.2435	0.2462
Pt-Au4	0.2569	0.2614	0.2321
Σ	1.0276	0.9783	0.9776

the z-axis (the original torus axis) have the strongest Pt–Au bonds. Upon introduction of this ligand these two sites become less and the cisoid Au atoms more strongly bonded to the central Pt atom. This observation is consistent with the well-known trans influences in mononuclear Pt compounds.

From Table 5 we can see that the smaller ^2J(Pt–P) coupling could be caused by the lower net radial overlap populations. Because the difference is only small (5%) some other effect may also influence this coupling.

Comparison of the orbital occupancies in the Pt atomic orbitals in the three molecules (Table 6) reveals a significant drop in occupancy of the s-orbital when the geometry is changed from toroidal to hemispherical and finally to that of the spherical carbonyl compound. An analogous difference is found when the hybridization of a C atom in, for example, hydrocarbons changes from sp^2 to sp^3. A reduction of 25% of the $^1J(^{13}C-^1H)$ coupling is expected on the basis of the difference in s orbital coefficients. The difference in the platinum s-orbital coefficients in the S^σ molecular orbital decreases from 0.2270 to 0.1459 upon addition of the CO to the toroidal cluster. On this basis one would expect the coupling constant to drop 36%, and the actual decrease is 22%.

Table 6 shows the low occupancy for the p_z orbital in both the toroidal and hemispherical geometries. The addition of the CO increases this occupancy through σ donation, and decreases the d_{xz} and d_{yz} occupation through $\pi^\star$ acceptance by the CO.

Table 6

Atomic orbital occupancies of the central metal in the S^σ MO

Pt	$Pt(AuPPh_3)_8$		$Pt(CO)(AuPPh_3)_8$ spherical
	toroidal	hemisphere	
s	0.616	0.554	0.522
p_x	0.273	0.282	0.284
p_y	0.273	0.268	0.257
p_z	0.042	0.034	0.382
$d_{x^2-y^2}$	1.784	1.863	1.867
d_{z^2}	1.974	1.846	1.600
d_{xy}	1.784	1.780	1.781
d_{xz}	1.861	1.935	1.764
d_{yz}	1.861	1.862	1.742

Acknowledgement

We would like to thank P. van Galen and M. Schoondergang for the elemental analysis and Dr. D.M.P. Mingos for providing facilities for the MO calculations. This research was supported by the Dutch organization for Scientific Research (NWO).

References

1 W. Bos, J.J. Bour, J.W.A. van der Velden, J.J. Steggerda, A.L. Casalnuovo, and L.H. Pignolet, J. Organomet. Chem., 253 (1983) C64.
2 W. Bos, R.P.F. Kanters, C.J. van Halen, W.P. Bosman, H. Behm, J.M.M. Smits, P.T. Beurskens, and J.J. Bour, J. Organomet. Chem., 307 (1986) 385.
3 R.P.F. Kanters, P.P.J. Schlebos, J.J. Bour, W.P. Bosman, H.J. Behm, and J.J. Steggerda, Inorg. Chem., 27 (1988) 4034.
4 J.W.A. van der Velden, J.J. Bour, W.P. Bosman, and J.H. Noordik, Inorg. Chem., 22 (1983) 1913.
5 F.A. Vollenbroek, Synthesis and Investigation of Gold Cluster Compounds. PhD thesis, University of Nijmegen, The Netherlands, 1979.
6 R.P.F. Kanters, P.P.J. Schlebos, J.J. Bour, W.P. Bosman, J.M.M. Smits, P.T. Beurskens, and J.J. Steggerda, Inorg. Chem., 29 (1990) 324.
7 J.J. Bour, R.P.F. Kanters, P.P.J. Schlebos, and J.J. Steggerda, Recl. Trav. Chim. Pays-Bas, 107 (1988) 211.
8 J.J. Steggerda, J.J. Bour, and J.W.A. van der Velden, Recl. Trav. Chim. Pays-Bas, 101 (1982) 164.
9 J.J. Bour, P.P.J. Schlebos, R.P.F. Kanters, W.P. Bosman, J.M.M. Smits, P.T. Beurskens, and J.J. Steggerda, to be published.
10 D.G. Evans and D.M.P. Mingos, J. Organomet. Chem., 232 (1982) 171.
11 D.M.P. Mingos, Proc. Roy. Soc. A, 308 (1982) 25.
12 D.M.P. Mingos and K.P. Hall, Prog. Inorg. Chem., 32 (1982) 239.
13 D.M.P. Mingos, K.P. Hall, and D.I. Gilmour, J. Organomet. Chem., 268 (1984) 275.